Chronic intermittent tachypacing by an optogenetic approach induces arrhythmia vulnerability in human engineered heart tissue

Marta Lemme[1,2], Ingke Braren[1,2], Maksymilian Prondzynski ⓘ [1,2†], Bülent Aksehirlioglu[1], Bärbel M. Ulmer[1,2], Mirja L. Schulze[1,2], Djemail Ismaili[3], Christian Meyer ⓘ [2,3], Arne Hansen[1,2], Torsten Christ ⓘ [1,2], Marc D. Lemoine ⓘ [1,2,3‡], and Thomas Eschenhagen ⓘ [1,2*,‡]

[1]Institute of Experimental Pharmacology and Toxicology, University Medical Center Hamburg-Eppendorf, Martinistrasse 52, 20246 Hamburg, Germany; [2]DZHK (German Centre for Cardiovascular Research), Partner Site Hamburg/Kiel/Lübeck, 20246 Hamburg, Germany; and [3]Department of Cardiology-Electrophysiology, University Heart Center, 20246 Hamburg, Germany

Aims	Chronic tachypacing is commonly used in animals to induce cardiac dysfunction and to study mechanisms of heart failure and arrhythmogenesis. Human induced pluripotent stem cells (hiPSC) may replace animal models to overcome species differences and ethical problems. Here, 3D engineered heart tissue (EHT) was used to investigate the effect of chronic tachypacing on hiPSC-cardiomyocytes (hiPSC-CMs).
Methods and results	To avoid cell toxicity by electrical pacing, we developed an optogenetic approach. EHTs were transduced with lentivirus expressing channelrhodopsin-2 (H134R) and stimulated by 15 s bursts of blue light pulses (0.3 mW/mm^2, 30 ms, 3 Hz) separated by 15 s without pacing for 3 weeks. Chronic optical tachypacing did not affect contractile peak force, but induced faster contraction kinetics, shorter action potentials, and shorter effective refractory periods. This electrical remodelling increased vulnerability to tachycardia episodes upon electrical burst pacing. Lower calsequestrin 2 protein levels, faster diastolic depolarization (DD) and efficacy of JTV-519 (46% at 1 μmol/L) to terminate tachycardia indicate alterations of Ca^{2+} handling being part of the underlying mechanism. However, other antiarrhythmic compounds like flecainide (69% at 1 μmol/L) and E-4031 (100% at 1 μmol/L) were also effective, but not ivabradine (1 μmol/L) or SEA0400 (10 μmol/L).
Conclusion	We demonstrated a high vulnerability to tachycardia of optically tachypaced hiPSC-CMs in EHT and the effective termination by ryanodine receptor stabilization, sodium or hERG potassium channel inhibition. This new model might serve as a preclinical tool to test antiarrhythmic drugs increasing the insight in treating ventricular tachycardia.

* Corresponding author. Tel: +49 40 7410 52180; fax: +49 40 7410 54876, E-mail: t.eschenhagen@uke.de
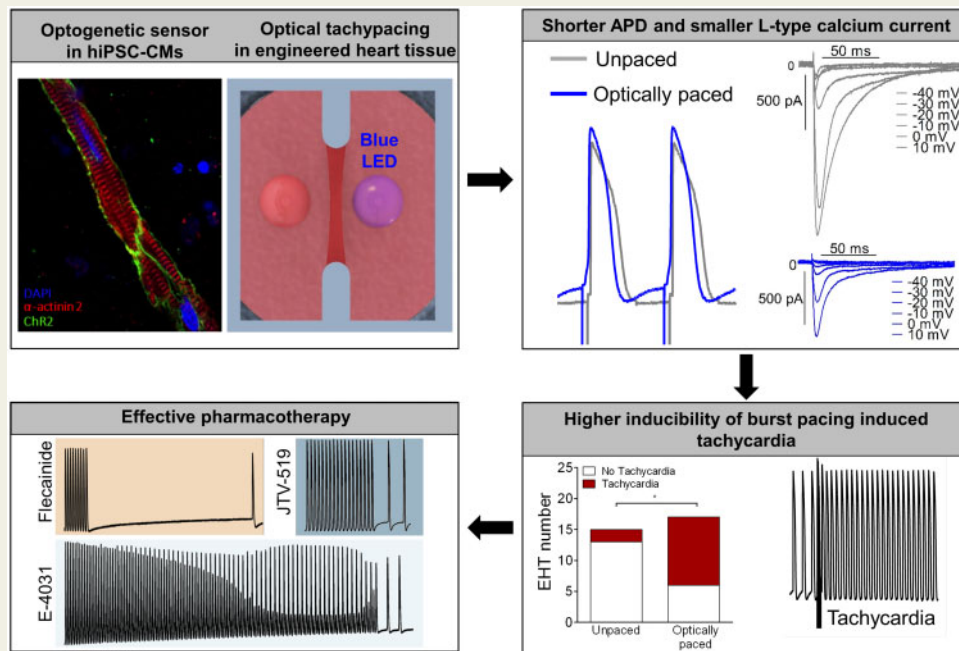
† Present address: Department of Cardiology, Boston Children's Hospital, Harvard Medical School, Boston, USA.

‡ These authors contributed equally.

Graphical Abstract

| Optogenetic sensor in hiPSC-CMs | Optical tachypacing in engineered heart tissue |
| Shorter APD and smaller L-type calcium current |

| Effective pharmacotherapy | Higher inducibility of burst pacing induced tachycardia |

1. Introduction

Chronic tachypacing is commonly used in animals to model human cardiac diseases. Pacing right atria of dogs and goats at 400 beats/min for 6 weeks induced sustained atrial fibrillation and atrial remodelling characterized by shortened action potential duration (APD) and shortened effective refractory period (ERP) associated with reduced Ca^{2+} current (I_{CaL}) density.[1,2] Ventricular tachypacing, e.g. pacing of the canine right ventricle with 240 beats/min for 3 weeks, induced signs of heart failure with inconsistent alterations of APD.[3,4] While these and other studies were instrumental in elucidating basic heart failure and arrhythmia mechanisms, differences in cardiomyocyte (CM) physiology between animals and humans,[5] including beating rate, energetics, Ca^{2+} cycling, myofilament composition, expression of key ion channels, and cellular electrophysiology especially in the repolarization phase of the action potential (AP) may be a limitation.[6] It would therefore be desirable to study mechanisms of electrical remodelling in human models. The recent advent of the human induced pluripotent stem cell (hiPSC) technology and an increasingly refined capacity to differentiate hiPSCs into disease-relevant cell types such as cardiomyocytes (hiPSC-CMs) provide an unprecedented opportunity to do so. Indeed, hiPSC-CM exhibit similar ion channel composition as native human CMs[7–9] and are increasingly used as a model for studying mechanisms of inherited cardiac diseases and for drug screening.[10,11] However, the use of hiPSC-CMs to model tachycardia-induced heart failure does not take into consideration hemodynamic and autonomic factors that are present in animal models.

Until now, electrical field stimulation has been mainly employed as a mean to improve hiPSC-CM maturation.[12–14] On the contrary, chronic electrical stimulation can also induce structural and electrophysiological adverse remodelling in hiPSC-derived ventricular CMs.[15] Rapid electrical pacing of hiPSC-CMs disturbed calcium homeostasis, which led to mitochondrial stress, promoted cell apoptosis, and caused electrophysiological remodelling.[16] The mechanisms of these adverse consequences of electrical pacing are not clear and may have also technical reasons. While electrical stimulation in intact animals can be done without temporal limitations, chronic pacing under *in vitro* conditions is complicated by irreversible Faradaic reactions. Negative effects of Faradaic reactions are the oxidation of electrodes, generation of chlorine and hydroxyl radicals, and formation of hypochlorous acid and chlorate.[17] Electrode charging in culture medium also raises the probability for water hydrolysis causing pH alterations.[18] These electrochemical reactions limit the efficacy and time span of application of electrical stimuli.[19] In this regard, light-sensitive ion channels represent an alternative to overcome this constraint. Channelrhodopsin-2 (ChR2) is a genetically targeted, light-activated non-selective cation channel used in optogenetics to modulate cell excitability. Once activated by blue light (470 nm), ChR2 allows the influx of cationic ions, mainly Na^+, consequentially depolarizing the membrane potential and generating APs.[20] ChR2 can also be applied for stopping arrhythmias. Constant illumination of ChR2-expressing CMs *in vitro* prolonged depolarization and refractoriness and electrically silenced illuminated areas.[21] However, it remains unknown how chronic optical tachypacing affects electrophysiology and function of

hiPSC-derived cardiac tissues. Therefore, the current study was conducted to evaluate the effect of chronic optical tachypacing on hiPSC-derived CMs in engineered heart tissue (EHT) format.[22] This system offers a more physiological cell environment and allows monitoring of the major parameters of heart function: force, pacemaking activity, contraction, and relaxation kinetics[22] as well as cardiac electrophysiology.[7]

2. Methods

An expanded method section is available in the Supplementary material online.

2.1 Differentiation of hiPSC-CMs and generation of EHTs

This investigation conforms to the principles outlined by the Declaration of Helsinki and the Medical Association of Hamburg. All materials from patients were taken with informed consent of the donors. All procedures involving the generation and analysis of hiPSC lines were approved by the local ethics committee in Hamburg (Az PV4798, 28 October 2014). Differentiation and generation of EHTs was performed as described before.[23] EHTs were transduced with EF1a-hChR2 (H134R, Supplementary material online, *Figure S1*) lentivirus during casting. Specifically, a multiplicity of infection (MOI) equal to 0.2 was used during EHT casting. Analysis of contractile force was performed by video-optical recording as previously described[22] on a set-up available from EHT Technologies. All data were confirmed in at least three batches.

2.2 AP recording

APs in EHT were recorded with sharp microelectrodes as previously described.[7] To investigate the effect of chronic optical tachypacing on electrical activity, APs were recorded from optically paced and unpaced ChR2 transduced EHTs (ChR2-EHTs, 28–35 days old) during spontaneous activity and under field-stimulation condition at a fixed rate (rectangular pulse of 0.5 ms, 50% above voltage threshold). APD, upstroke velocity (dV/dt_{max}), take-off potential (TOP) and ERP were analysed with the Lab-Chart software (ADInstruments, Spechbach, Germany). All parameters related to APD were corrected for the beating rate with Bazett correction.[24] During AP recording, a maximum of 20 attempts of burst pacing [cycle length (CL) 50 ms, pacing duration 300–500 ms] was used to induce tachycardia. Reversion of tachycardia was attempted with: burst pacing (CL 50 ms, pacing duration 100–200 ms), illumination with blue light for 500 ms (at 0.3 mW/mm^2) and drug exposure. Different drugs with potential antiarrhythmic action were applied during a stable tachycardia in order to terminate these tachycardia episodes: ivabradine (1 µmol/L), flecainide (1 µmol/L), JTV-519 (1 µmol/L), SEA0400 (10 µmol/L), and E-4031 (1 µmol/L). Incubation time of the antiarrhythmic drugs was >15 min.

2.3 Statistics

Statistical analyses were performed with GraphPad Prism software 5.0. Data are expressed as mean ± SEM in bar graphs and scatter plots. Differences between groups were analysed by unpaired and paired *t*-test when appropriate. The incidences of tachycardia were compared using Fisher's exact probability test. Results were considered statistically significant if the *P*-value was <0.05. Replicates were expressed as *n* = EHT number/batch number. All experiments to study the effect of chronic optical tachypacing consist of three independent batches.

3. Results

3.1 Establishment of the model

To allow simultaneous application of blue light and contractility recording of EHTs, we successfully refined a commercially available platform (EHT Technologies GmbH, Hamburg[22]). The standard array with 24 white light-emitting diodes (LED) was replaced by a custom-made plate that contained 24 red LEDs (NSPR510CS Nichia, λ = 700 nm, Tokushima Japan) and 24 blue LEDs (NSPB510BS Nichia, λ = 470 nm). The plate with LEDs was mounted 8 mm below the bottom of the 24-well plate in a way that the red/blue LEDs were positioned left/right of the centre of each well and thereby of each EHT suspended in the 24-well plate above (*Figure 1*). Red LEDs were turned on during contractility recording to allow the camera to visualize the beating EHT. Blue LEDs were used for the optical pacing of ChR2 transduced EHTs. The platform was controlled by a trigger box, which was connected to an external stimulus generator (S88X Dual Output Square Pulse Stimulator, *Figure 1*). The trigger box enabled us to switch on/off and to manipulate the intensity of the red and blue LEDs, while the stimulus generator was used to define the waveform of the blue light pacing. The platform containing the 24-well plate with the EHTs and the bottom plate with the LEDs was placed in a standard cell culture incubator (37 °C, 40% O_2, 7% CO_2) during optical tachypacing of the ChR2 transduced EHTs.

EHTs were casted from hiPSC-CMs with a percentage of cardiac troponin-T (cTnT)-positive cells of 91.6 ± 2.9% (*n* = 3 batches). As previously reported,[8,25] repolarization fraction (APD_{90}-APD_{50})/APD_{90} was used as a discriminator between ventricular and atrial CMs. HiPSC-CMs used in this study for EHT casting were predominantly ventricular-like CMs characterized by a repolarization fraction of 0.22 ± 0.01 (*n* = 13 EHTs). In the EHT format, hiPSC-CMs form a synchronously beating syncytium which generates auxotonic contractile force by deflecting two elastic silicone posts.[22,23] Transduction with ChR2-lentivirus of hiPSC-CMs during EHT casting did not principally interfere with EHT generation (>90% of EHTs formed functional contracting tissues, 32/33), but ChR2 transduced EHTs (ChR2-EHTs) showed a later onset of spontaneous beating (7.5 ± 0.2 days vs. 4.8 ± 0.2 days, *n* = 20/2) and a higher spontaneous beating rate (2.3 ± 0.1 Hz vs. 1.2 ± 0.03 Hz, *n* = 20/2) than non-transduced EHTs. ChR2-eYFP transduction efficiency in EHTs was quantified by flow cytometry analysis. At an MOI equal to 0.2, 25.7 ± 0.6% (*n* = 4/2) of cells within the EHT were ChR2-YFP positive (*Figure 2A*). The photosensitive protein was mainly localized at the sarcolemma of the hiPSC-CMs (*Figure 2B*). Immunofluorescence analysis showed that ChR2 was still expressed and localized at the sarcolemma at Day 28 after transduction (*Figure 2B*).

3.2 ChR2-EHTs follow optical pacing

The spontaneous beating rate of Ctrl-EHTs (non-transduced with ChR2-lentivirus) was unaffected by light pacing (*Figure 2C*, Supplementary material online, *Video S1*), while ChR2-EHTs followed pacing (*Figure 2C*, Supplementary material online, *Video S2*) from 2 to 5 Hz with 30 ms light pulses at 0.3 mW/mm^2. ChR2-EHTs showed an increase in force compared to their spontaneous beating rate (~1.9 ± 0.05 Hz, *n* = 15) until 2 Hz pacing. From 2 to 5 Hz ChR2-EHTs showed an inverse force–frequency relationship.[25] The force decreased from 0.12 ± 0.004 mN at 2 Hz to 0.07 ± 0.003 mN at 5 Hz (*n* = 15, *Figure 2D*). As expected, the contraction kinetics accelerated at higher frequencies. $TTP_{-80\%}$ and $RT_{80\%}$ decreased from 95.5 ± 1.4 ms at 2 Hz to
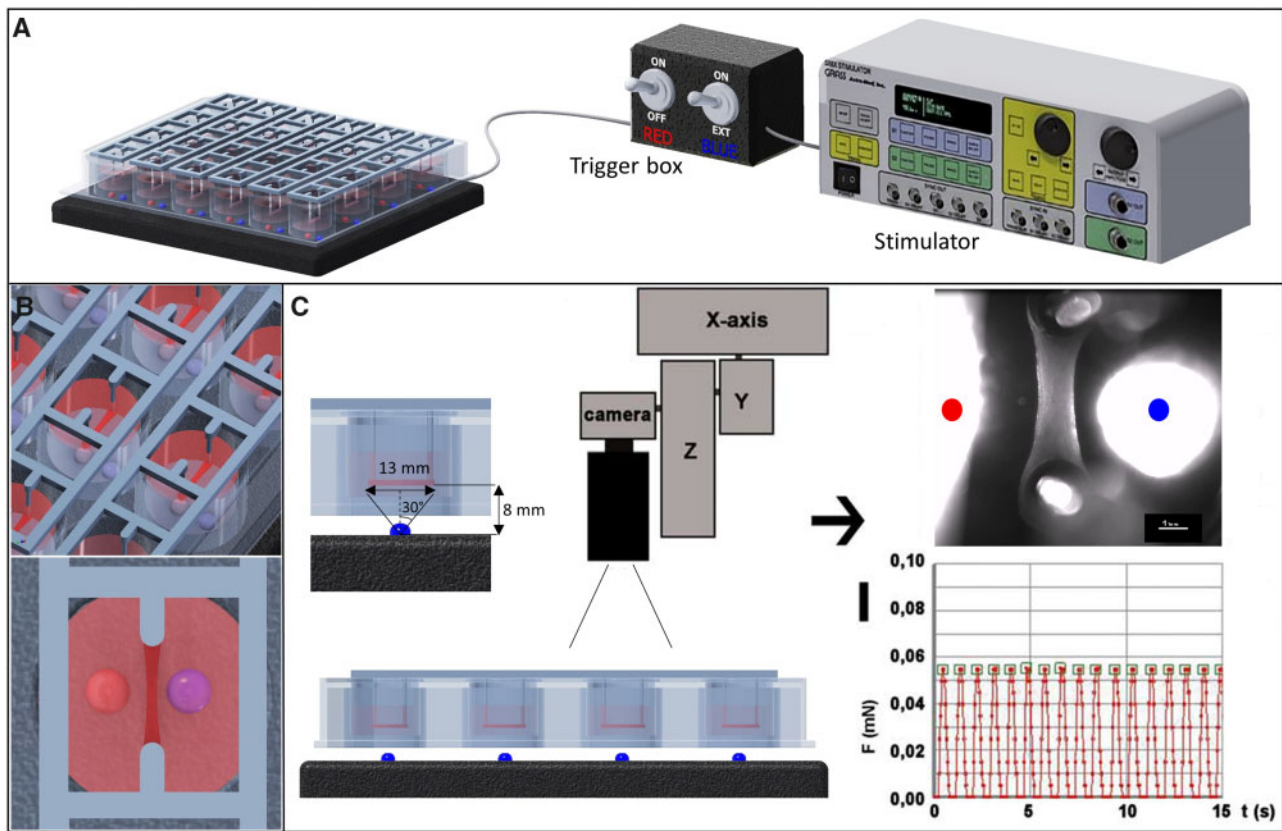
Figure 1 Custom-made system for optical pacing. (A) Optogenetic platform containing 24 red and blue light-emitting diodes (LEDs) for mounting a 24-well plate containing ChR2 transduced EHTs (left). This platform can be placed inside the incubator to perform chronic optical tachypacing. Red and blue LEDs were used for visualization and optical pacing of the EHTs, respectively. The platform was controlled by a trigger box, which was connected to an external stimulus generator. The trigger box enabled to switch on/off and to manipulate the intensity of LEDs, while the external stimulus generator was used to define the waveform of the blue light pacing. (B) View from the top of the 24-well plate. EHTs were positioned between the red and blue LEDs. (C) Cross-section of the optogenetic platform (left) to visualize the distance between the blue LED and the EHT, as the system to perform video-optical contraction analysis of EHTs (right).

77.3 ± 1.6 ms at 5 Hz and from 116.0 ± 1.6 ms at 2 Hz to 83.5 ± 2.3 ms at 5 Hz, respectively (*Figure 2D*).

3.3 Establishment and validation of the optogenetic platform for chronic tachypacing

To characterize the custom-made optogenetic system, a strength–duration curve of optical pacing threshold was constructed by varying pulse duration (5–100 ms) and light intensity/irradiance (0.003–0.3 mW/mm^2, Supplementary material online, *Figure S2*). Continuous light pacing induces desensitization which reduces the consistency of depolarization.[26] In line with these observations, we found that 7 days of continuous 3 Hz optical tachypacing led to loss of capture in EHTs. We therefore chose a repetitive train stimulation protocol at the maximal irradiance achievable with our set-up (0.3 mW/mm^2). Light pulse duration and pulse rate were set at 30 ms and 3 pulses/s, respectively. This optical interval pacing protocol of 15 s bursts at 3 Hz separated by 15 s without pacing was applied to ChR2-EHTs for 3 weeks, starting 7 days after casting.

3.4 Chronic optical tachypacing evokes faster contraction kinetics in EHTs

Contractility measurements of optically paced and unpaced ChR2-EHTs were performed at Day 28 (*Figure 3*). Chronic interval pacing accelerated the contraction kinetics of the EHTs (*Figure 4*). TTP$_{-80\%}$ decreased from 128.5 ± 1.6 ms to 118.7 ± 1.8 ms (*P* < 0.001, unpaired *t*-test; *n* = 16/3, *Figure 4C*). Chronic optical tachypacing also induced RT$_{80\%}$ shortening from 154.0 ± 5.0 ms to 132.0 ± 2.4 ms (*P* < 0.001, unpaired *t*-test; *n* = 16/3, *Figure 4D*). Spontaneous beating rate and force were not affected by the chronic tachypacing (*Figure 4A* and *B*).

3.5 Chronic optical tachypacing induces APD$_{90}$ shortening and L-type Ca^{2+} current reduction

After 3 weeks of optical interval pacing at 3 Hz, APs of optically paced and unpaced ChR2-EHTs were elicited by field stimulation (2 Hz). APD$_{90}$ of optically paced ChR2-EHTs was shorter than that of unpaced ChR2-EHTs (176.6 ± 5.6 ms vs. 205.6 ± 6.4 ms, *n* = 16/3 vs. 14/3; *P* = 0.007, unpaired *t*-test, *Figure 4H*). In line with the changes in APD, ERP was shorter in the optically paced than in the unpaced ChR2-EHTs
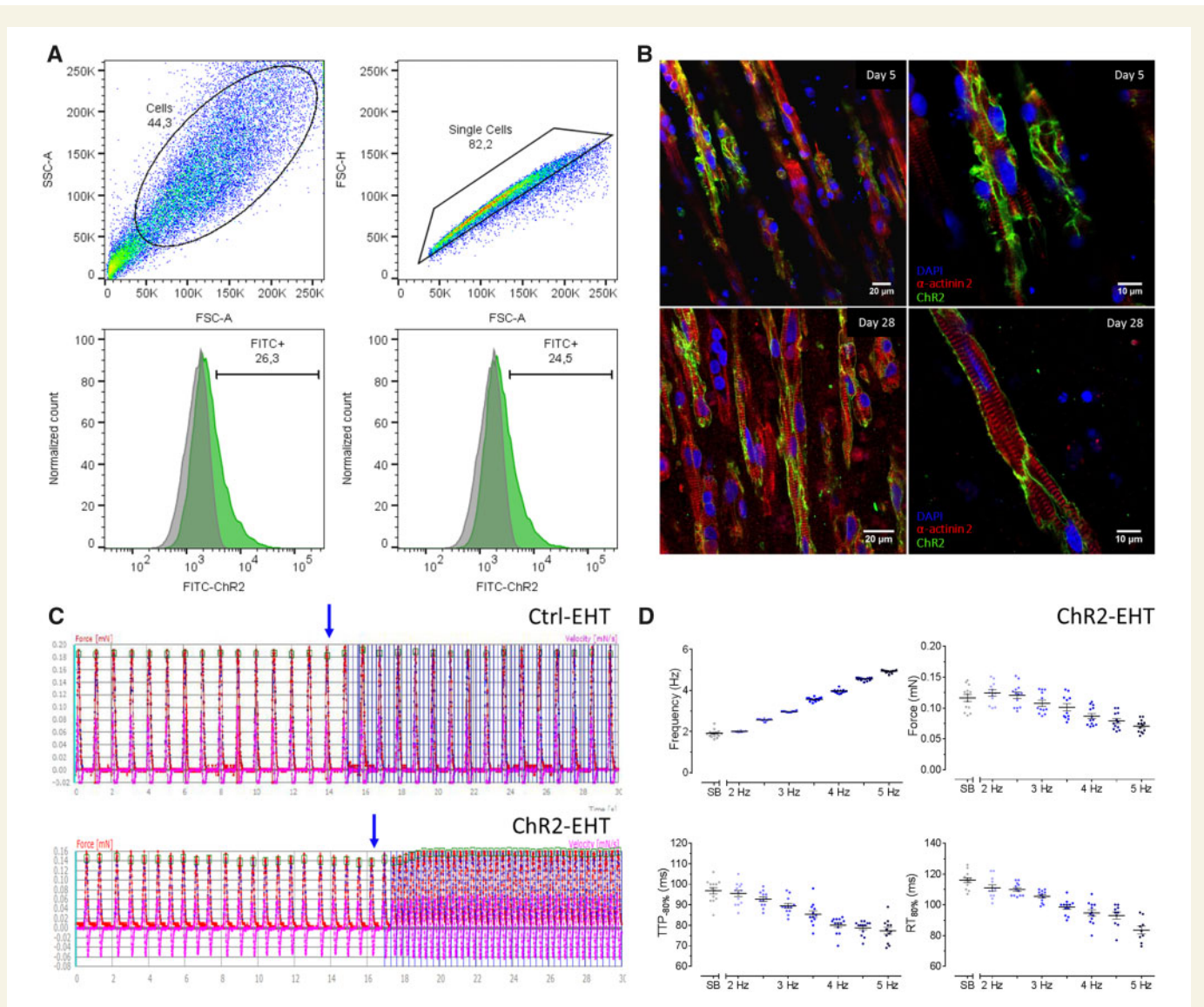
Figure 2 Stable ChR2 transduction allows optical pacing of EHTs. (*A*) Representative FACS analyses showing ChR2 transduction efficiency with multiplicity of infection (MOI) of 0.2. ChR2 positive (FITC$^+$) hiPSC-CMs were determined by the difference between the green peak (ChR2 transduced EHTs) and the grey peak (non-transduced EHTs). (*B*) Immunofluorescence of ChR2 (green), α-actinin 2 (red), and DAPI (blue) of ChR2-EHTs at 5 and 28 days after transduction. (*C*) Original recordings of contractions over time (30 s) in Ctrl- and ChR2-EHTs; green squares indicate automatically identified contractions used for calculating beating frequency, force, and times of contraction and relaxation. The graphs showed regular beating pattern under spontaneous beating (SB) and under optical pacing (blue arrow represent the start of optical pacing). (*D*) Summary of contraction parameters measured in ChR2-EHTs while optical pacing rate was increased acutely. Data are expressed as mean ± SEM. *n* = 15/2, with *n* = number of EHTs/number of batches.

(199.6 ± 7 ms vs. 232.5 ± 6 ms, *n* = 16 to 14/3; *P* = 0.002, unpaired *t*-test, *Figure 4I*). The optically paced ChR2-EHTs showed less negative TOP (-66.3 ± 0.7 mV vs. -72.8 ± 1 mV, *n* = 16 to 14/3; *P* < 0.001, unpaired *t*-test, *Figure 4E*), lower dV/dt_{max} (38.9 ± 4.2 V/s vs. 89.6 ± 17.8 V/s, *n* = 16 to 14/3; *P* < 0.001, unpaired *t*-test, *Figure 4F*) and smaller action potential amplitude (APA, 89.5 ± 2.2 mV vs. 102.2 ± 3.6 mV, *n* = 16 to 14/3; *P* = 0.007, unpaired *t*-test, *Figure 4G*). To study whether APD shortening may result from lower Ca^{2+} current we performed patch clamp experiments. CMs isolated from optically tachypaced ChR2-EHTs showed lower cell capacitance than CMs from unpaced ChR2-EHTs indicating tachypacing-induced remodelling (cell capacitance: 38.6 ± 4 pF vs. 56.7 ± 4.5 pF, *n* = 17/3 vs. 20/3, *P* = 0.006, unpaired *t*-test, Supplementary material online, *Figure S3*). However, Ca^{2+} current amplitudes were

much smaller than to be expected from lower cell size, giving Ca^{2+} current densities of 5.6 ± 1.0 pA/pF vs. 13 ± 1.4 pA/pF, *n* = 17/3 vs. 20/3, *P* < 0.001, unpaired *t*-test, *Figure 6E*).

3.6 Chronic optical tachypacing increases tachycardia inducibility

To evaluate whether chronic interval pacing also affected arrhythmia vulnerability, EHTs were subjected to a burst pacing protocol (*Figure 3B*). In accordance to clinical electrophysiology,[27] electrical burst pacing (20 Hz, ~500 ms) induced a sustained tachycardia episode in some EHTs, during which the EHT beat spontaneously with a shorter CL of 215 ± 8 ms (~4.5 Hz; *n* = 13/3) compared to the basal rate (CL 702 ± 100 ms,
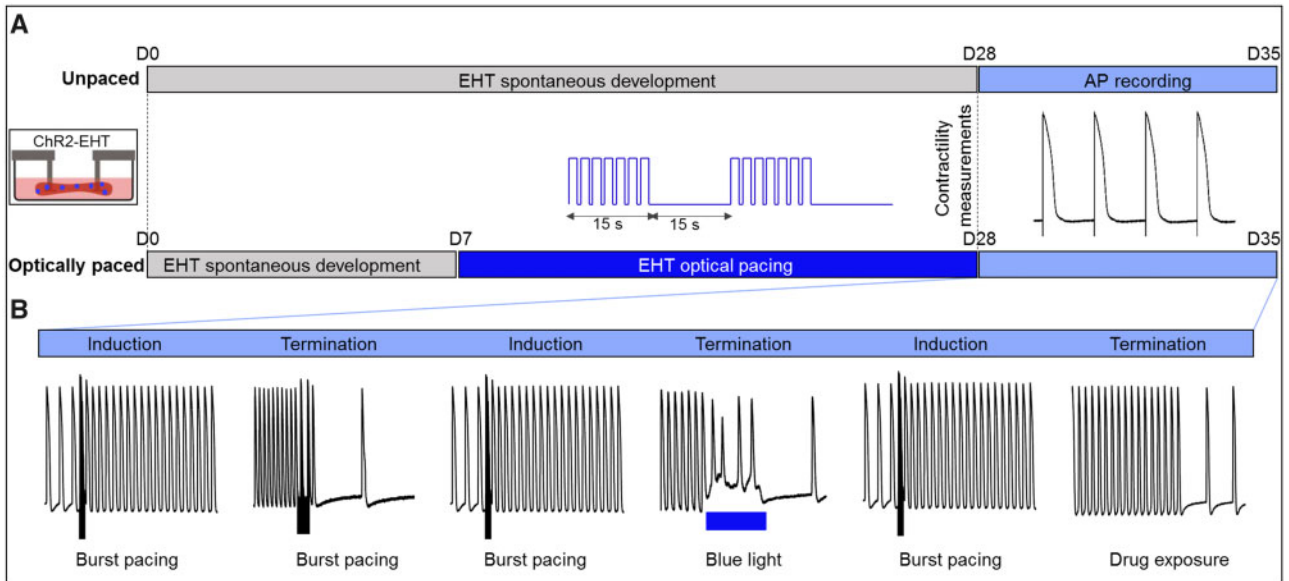
Figure 3 Protocol for chronic optical tachypacing of ChR2-EHTs. (*A*) Schematic protocol for studying the effect of chronic optical tachypacing on ChR2-EHTs. ChR2-EHTs included in the optically paced group were paced for 3 weeks with 15 s burst at 3 Hz followed by 15 s without pacing. From Day 28 functional analyses (contractility and action potential) of optically paced vs. unpaced ChR2-EHTs were performed. (*B*) Protocol to induce sustained tachycardia episodes by 20 Hz burst pacing and to terminate these episodes with different interventions.
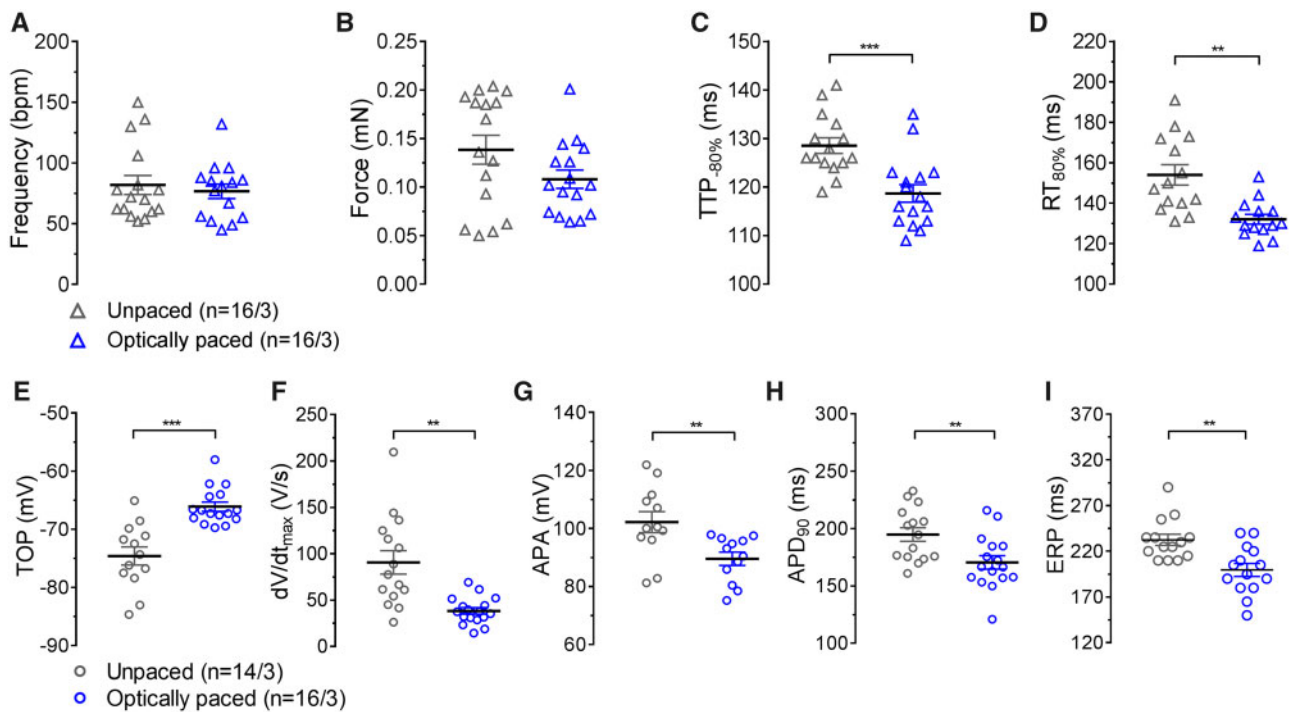

Figure 4 Chronic optical tachypacing affects contraction and action potential of ChR2-EHTs. Contractions: frequency (*A*), force (*B*), contraction (*C*), and relaxation time (*D*) of unpaced and optically paced ChR2-EHTs measured at Day 28. Action potentials: mean values for take-off potential (TOP) (*E*), upstroke velocity (dV/dt_{max}) (*F*), action potential amplitude (APA) (*G*), APD_{90} (*H*) and effective refractory period (ERP) (*I*) of optically paced vs. unpaced ChR2-EHTs were measured from Days 28 to 35. APs were recorded at 37°C under electrical field stimulation at 2 Hz. Data are expressed as mean ± SEM (**$P < 0.01$, ***$P < 0.001$, unpaired *t*-test; $n = 14$–16/3, with n = number of EHTs/number of batches).
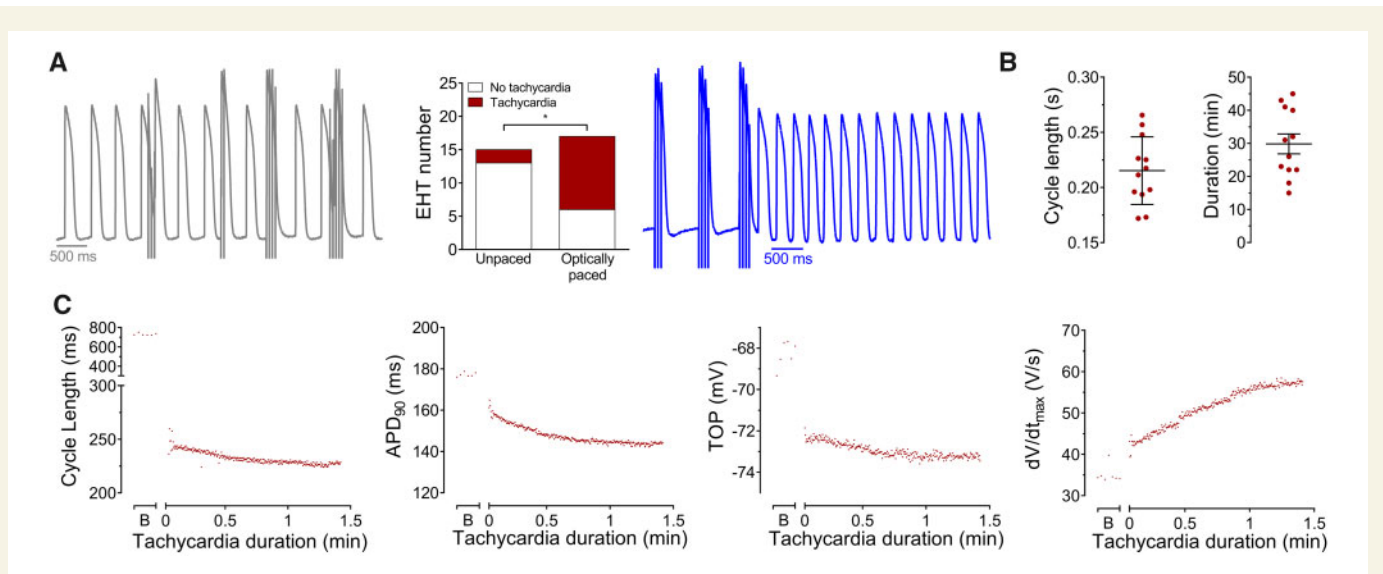
Figure 5 Tachycardia induction in ChR2-EHTs. (A) Fraction of EHTs in which tachycardia could be induced by 20 Hz burst pacing (red) in unpaced and optically paced EHTs (*$P < 0.05$, Fisher's exact test; $n = 15–17/3$ EHTs). Representative traces of successful and unsuccessful tachycardia induction attempts by burst pacing. (B) Mean values of cycle length and duration of tachycardia episodes. Data are expressed as mean ± SEM, $n = 13/3$, with $n =$ number of EHTs/number of batches. (C) Averaged cycle length, APD_{90}, upstroke velocity and take-off potentials obtained from six EHTs during spontaneous baseline (B) and during the first min of tachycardia episodes.

~1.4 Hz, $n = 13/3$, $P < 0.001$, paired t-test). Optically paced EHTs showed burst pacing-induced tachycardia in 64% of cases (11/17), while unpaced EHTs only in 13% (2/15; *Figure 5A*). Tachycardia episodes did not differ qualitatively between optically paced and unpaced ChR2-EHTs. They showed a mean duration of 29.8 ± 2.9 min (*Figure 5B*). After induction, the tachycardia accelerated with CL decreasing from 249 ± 3 ms to 230 ± 4 ms (*Figure 5C*). APD_{90} decreased from 161 ± 15 ms to 144 ± 13 ms, similar to values under normal paced conditions (*Figure 5C*). Interestingly, within 1.5 min from tachycardia induction the upstroke velocity increased from 43 ± 10 V/s to 58 ± 11 V/s, paralleled by lowering of TOP (*Figure 5C*). After the first 1.5 min from tachycardia induction, upstroke velocity and TOP remained stable until the end of tachycardia (Supplementary material online, *Figure S4c*). Tachycardia episodes demonstrated a time-dependent decrease in CL variability calculated as the CL standard deviation of 50 consecutive tachycardia beats (Supplementary material online, *Figure S4b*). This observation mirrors an electrophysiological study with ventricular tachycardia in humans.[28] Stability of tachycardia episodes was confirmed by Poincaré plots[29] of CL, showing the relationship of the RR intervals vs. the next RR interval (Supplementary material online, *Figure S4a*).

3.7 Chronic optical tachypacing induces faster DD

Optically paced ChR2-EHTs showed faster DD at 2 Hz field stimulation (*Figure 6A*). The higher DD was weakly correlated with higher AP firing rate (Supplementary material online, *Figure S5*). The weakness of correlation is in accordance with unaltered spontaneous contraction rate in chronically paced EHTs (*Figure 4A*). At 2 Hz field stimulation, DD was 28 ± 4 mV/s ($n = 17/3$) in optically paced ChR2-EHTs compared to 10 ± 3 mV/s in unpaced ChR2-EHTs ($n = 15/3$) (*Figure 6B*). This was not associated with increased gene expression of pacemaker channels, as mRNA-levels of HCN4 after chronic tachypacing were only 57 ± 15% of

control. mRNA-levels of SLC8A1 were slightly higher (110 ± 2% of control) and CACNA1C mRNA-levels did not differ between the groups (*Figure 6D* and Supplementary material online, *Figure S6*). EHTs in which tachycardia could be induced showed higher DD than EHTs in which tachycardia was not inducible (31 ± 4 mV/s vs. 7 ± 3 mV/s, $n = 13–19/3$, $P < 0.001$, unpaired t-test). Of note, EHTs with chronic tachypacing showed 41% higher mRNA-levels of CASQ2 in comparison to unpaced EHTs ($n = 6/3$, $P = 0.04$, unpaired t-test, *Figure 6D*), but 49% lower protein level of CASQ2 ($n = 6/3$, $P = 0.008$, unpaired t-test, *Figure 6F*), respectively. This apparently contradictory finding was confirmed by immunofluorescence staining for CASQ2 (*Figure 6F*). In order to elaborate mechanisms of remodelling we measured protein levels of key players in electromechanical coupling. Protein levels of sarco/endoplasmic reticulum Ca^{2+}-ATPase (SERCA) were unaltered while those of sodium calcium exchanger (NCX) were decreased in optically tachypaced compared to unpaced ChR2-EHTs (Supplementary material online, *Figure S7*). Phosphorylation of Ca^{2+}/calmodulin-dependent protein kinase II (CaMKII) at Thr286 was decreased in optically tachypaced compared to unpaced ChR2-EHTs (Supplementary material online, *Figure S7*).

3.8 Flecainide, JTV-519, and E-4031 terminated tachycardia

If tachycardia was inducible in ChR2-EHTs, it was sustained for a mean of 30 min (*Figure 5B*) and could be re-initiated by another burst pacing for several times. This allowed us to test different interventions to terminate these episodes. Tachycardia was terminated effectively and repeatedly by burst pacing applied by field electrodes[30] or by continuous illumination with blue light (*Figures 3B and 7*). In contrast to the effect on spontaneous beating rate of EHTs,[9] ivabradine exposure (1 μmol/L, 15 min of incubation) did not terminate tachycardia episodes, neither in optically paced ChR2-EHTs, nor in the small number of unpaced ChR2-EHT where tachycardia could be induced. SEA0400 induced ~20%
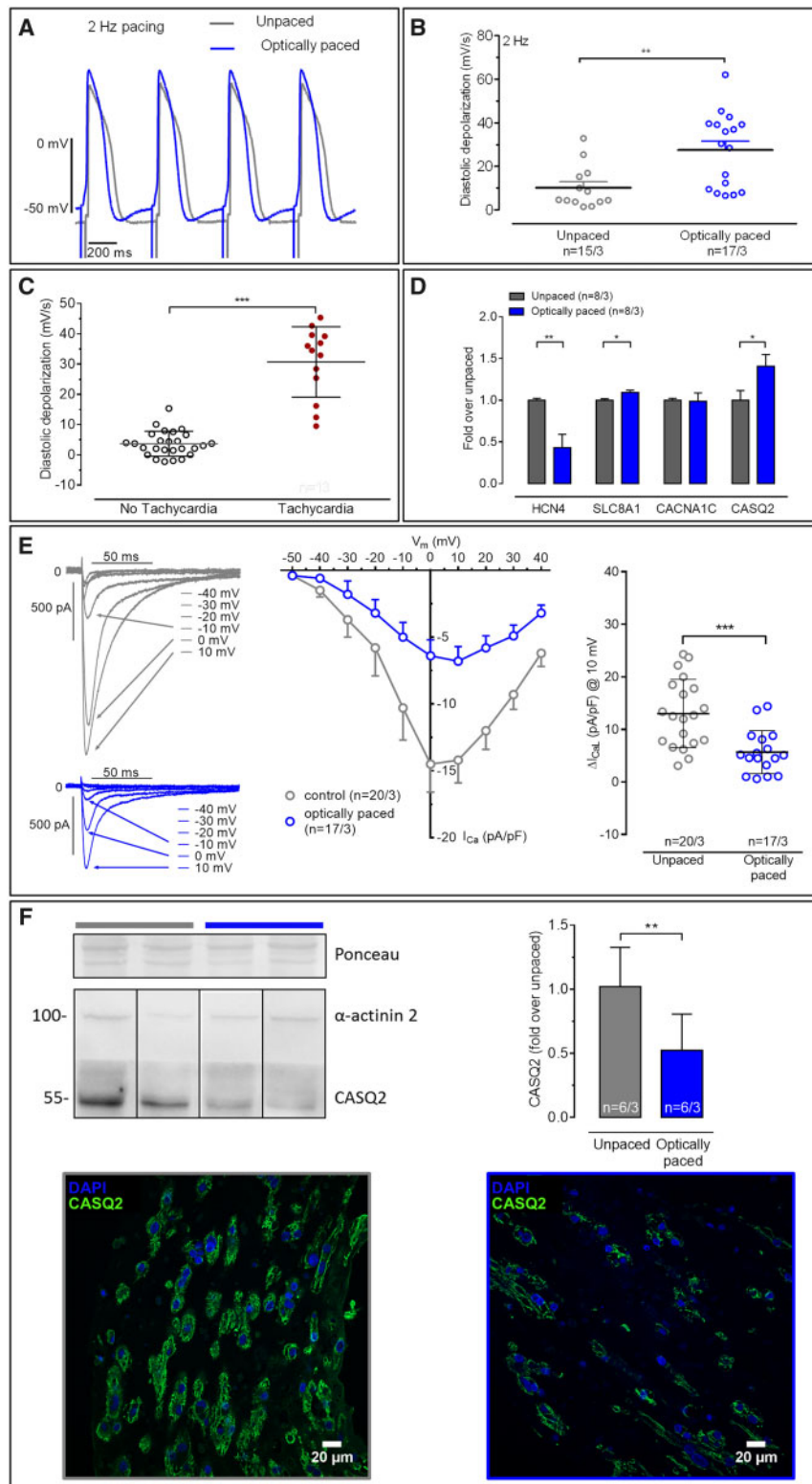
Figure 6 Tachycardia inducibility is associated with higher diastolic depolarization and lower CASQ2. (A) Comparison of representative AP traces of optically paced vs. unpaced ChR2-EHTs during 2 Hz field stimulation. (B) Quantification of diastolic depolarization of optically paced vs. unpaced ChR2-EHTs at 2 Hz (unpaired t-test; n = 15–17/3). (C) Quantification of diastolic depolarization in EHTs where tachycardia could or could not be induced (unpaired t-test; n = 19–13/3). (D) The mRNA-levels of HCN4, SLC8A1, CACNA1C, and CASQ2 of optically paced and unpaced ChR2-EHTs were normalized to housekeeping genes, and related to the unpaced group (unpaired t-test; n = 8/3). (E) Patch clamp measurements of I_{CaL} with representative tracings (left), IV-curves (middle) and quantification of I_{CaL} upon a depolarization from -80 to 10 mV in optically paced (blue) and unpaced (grey) ChR2-EHTs. (F) Protein level of CASQ2 was detected by western blot and normalized to α-actinin 2 level (unpaired t-test; n = 6/3). Immunofluorescence of CASQ2 (green) and DAPI (blue) of optically paced vs. unpaced ChR2-EHTs. Data are expressed as mean ± SEM with n = number of EHTs/number of batches; *P < 0.05, **P < 0.01, ***P < 0.001.

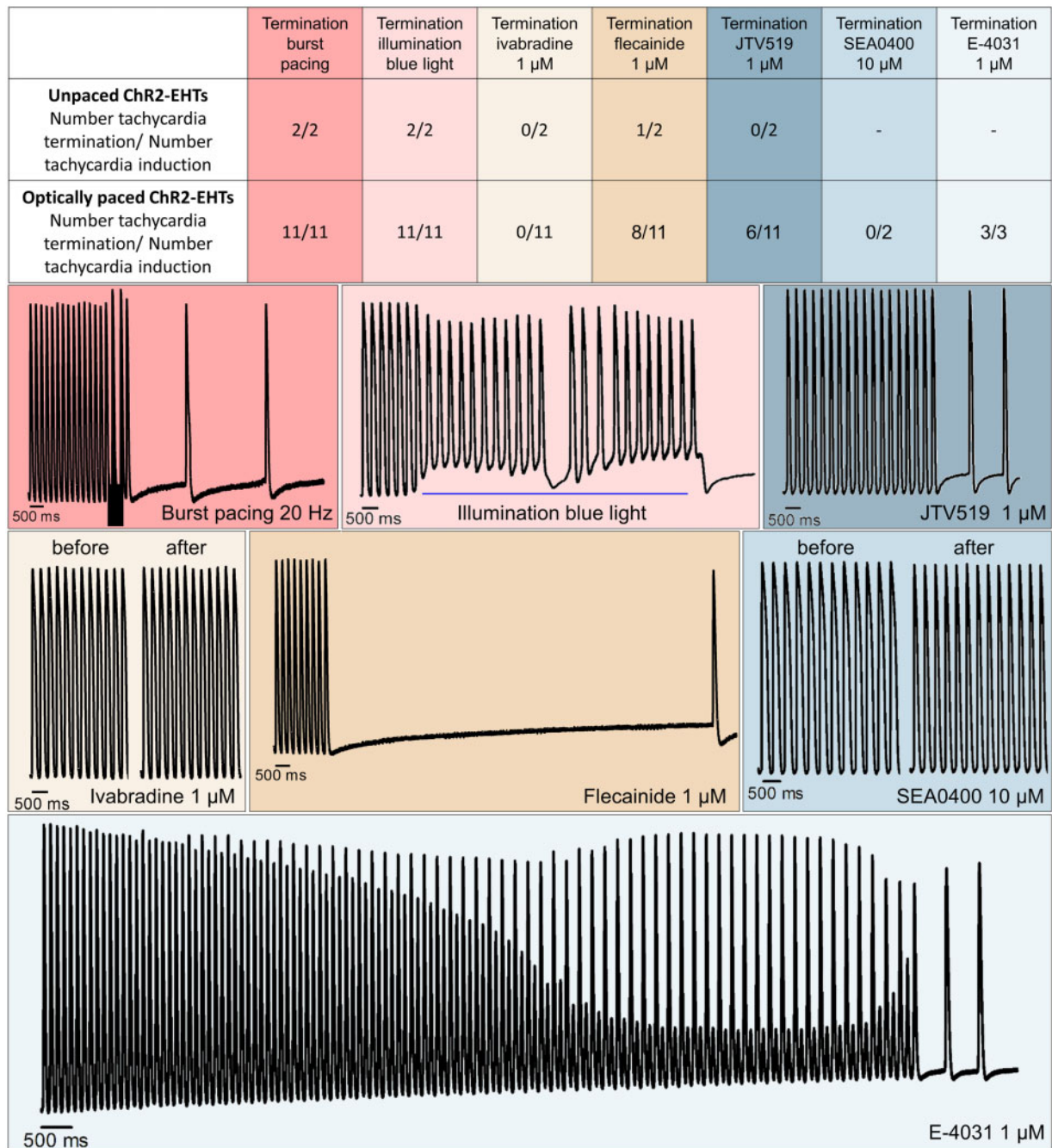|	Termination burst pacing	Termination illumination blue light	Termination ivabradine 1 µM	Termination flecainide 1 µM	Termination JTV519 1 µM	Termination SEA0400 10 µM	Termination E-4031 1 µM
Unpaced ChR2-EHTs Number tachycardia termination/ Number tachycardia induction	2/2	2/2	0/2	1/2	0/2	-	-
Optically paced ChR2-EHTs Number tachycardia termination/ Number tachycardia induction	11/11	11/11	0/11	8/11	6/11	0/2	3/3

Figure 7 Tachycardia termination in ChR2-EHTs. Burst pacing and blue light illumination showed maximum tachycardia termination efficiency. Exposure to ivabradine (1 µmol/L) for 15 min could not terminate tachycardia. Flecainide (1 µmol/L), E-4031 (1 µmol/L), and JTV-519 (1 µmol/L) showed 69, 100, and 46% efficacy in termination of tachycardia after 15 min exposure, respectively, while SEA0400 (10 µmol/L) did not terminate tachycardia episodes.

shortening of APD_{90}. SEA0400 (10 µM) was tested in two optically paced ChR2-EHTs, but it did not terminate tachycardia (*Figure 7*). The class Ic antiarrhythmic flecainide (1 µmol/L) terminated tachycardia in 69% of the EHTs after 4.3 ± 1.4 min, the ryanodine receptor-stabilizing drug JTV-519 (1 µmol/L) terminated tachycardia in 46% of the EHTs after 5.5 ± 1.5 min (*Figure 7*). The hERG potassium channel blocker E-4031 (1 µmol/L) prolonged APD_{90} by 32% and all three episodes of tachycardia were successfully terminated by E-4031 (*Figure 7*).

4. Discussion

4.1 EHT as a model for optical pacing

ChR2 has been successfully integrated into CMs in small animal models[31,32] and in monolayers of neonatal rat atrial myocytes[33] and hiPSC-CM.[34] Here we combined the advantages of the optogenetic approach with the advantage of the EHT system, which provides a 3D functional syncytium, promotes maturation of hiPSC-CMs and is stable over several

weeks. Blue light illumination of ~50 myocytes was required to induce *in vivo* optical pacing of transgenic mice.[20] In line with this finding, lentivirus at an MOI of 0.2 that transduced one-fourth of CMs in EHTs (*Figure 2A*) produced light-sensitive, homogenously contracting tissues. Lentiviral ChR2 expression slowed down EHT development (start of spontaneous beating) and increased spontaneous beating rate. The initially unexpected finding is in accordance with a recent observation that lentiviral transduction and ChR2 expression in neonatal rat ventricular myocytes increased spontaneous beating rate, induced adverse morphological changes, and lowered cell viability.[35] However, in our system, it did not affect maximum force development or CM or tissue structure when compared to non-transduced controls, rather reflecting the results of transgenic ChR2 expression in mice that was devoid of changes in heart rate or cardiac structure.[20] It was notable, though, that maximum diastolic potential was less negative and action potential upstroke velocity was lower than what we had observed previously in control EHTs.[9] These data indicate that expression of ChR2 in hiPSC-CMs has some background effects even if not illuminated that may be due to incomplete closure of the channel. Nevertheless, effects appear small and did not interfere with stable tissue formation and force generation of EHTs.

Importantly, blue light illumination consistently paced ChR2 transduced EHTs but was without effect in non-transduced controls. Pacing followed the expected dependency on light intensity, light pulse duration, and frequency up to 5 Hz. The lower limit of pacing frequency was around 1.8 Hz and attributed to the spontaneous beating rate. According to previous data, pacing between 1.8 and 2 Hz revealed a small positive force–frequency relationship, higher rates were associated with progressively decreasing force. These data indicate normal behaviour of the ChR2-transduced EHTs compared to previously published data.[25] Chronic continuous tachypacing led to quick desensitization and lack of capture, a phenomenon observed previously.[26,36] Therefore, it was necessary to establish an interval tachypacing protocol that allowed long-term pacing with complete capture over 3 weeks. The comparison between lentivirally transduced ChR2-EHTs with and without chronic tachypacing allowed us to distinguish the effects on cardiac function caused by the chronic optical tachypacing from the effects caused by the transduction. Therefore, ChR2-EHTs can be considered a suitable model to investigate effects of chronic optical tachypacing.

4.2 Electrical remodelling of EHT upon chronic optical tachypacing

ChR2-EHTs subjected to 3 weeks optical tachypacing showed faster spontaneous contraction kinetics, indicating remodelling (*Figure 4C* and *D*). Indeed, optical stimulation conditioned the contraction kinetics of CMs in a way that even after the removal from stimulation the spontaneous contraction kinetics remained adapted to the fast optical stimulus, similarly to previous reports.[37] Faster contraction kinetics were accompanied by shorter APD_{90} (*Figure 4H*) upon chronic optical tachypacing, as it was previously reported for chronic electrical stimulation.[15,37] Expression analysis did not reveal significant changes in the expression of depolarizing (*CACNA1C*) or repolarizing ion channels (*KCNH2* and *KCNQ1; Figure 6D* and Supplementary material online, *Figure S6*). Although transcript levels of *CACNA1C* were unchanged, APD_{90} shortening might be explained by lower I_{CaL} density in optically tachypaced compared to unpaced ChR2-EHTs (*Figure 6E*). The discrepancy between transcript levels of CACNA1C and Ca^{2+} current amplitude was previously observed[38] and points to additional changes in subunit expression and/or channel trafficking. Reduction of I_{CaL} with subsequent shortening

of APD is a typical finding in atria remodelled by tachypacing,[2,39] while ventricular models showed inconsistent alterations of APD but unaltered I_{CaL}.[40]

In addition, the lower Ca^{2+} influx via L-type Ca^{2+} channels might be also responsible for the decreased autophosphorylation of CaMKII at Thr286 (Supplementary material online, *Figure S7*). In line with these findings, the lower protein level of NCX may indicate a balanced adaptation to a decrease in I_{CaL}.[41] Lower autophosphorylation of CaMKII at Thr286, less I_{CaL} and less NCX all argue against Ca^{2+} overload and point to other arrhythmia mechanisms in our model.

Similar to contraction kinetics and APD_{90}, TOP was consistently less negative after chronic optical tachypacing than in unpaced controls (*Figure 4F*) and remained so even if the stimulation was stopped, again indicating remodelling. On the mRNA-level we observed a decrease of *KCNJ3* and *KCNJ5*, encoding the acetylcholine activated potassium current (Supplementary material online, *Figure S6*) and an increase in *SLC8A1* (*Figure 6D*), encoding for NCX, however protein levels of NCX were reduced (Supplementary material online, *Figure S7*).

In addition, TOP was depolarized in optically paced EHTs. The difference in TOP could underlie the lower upstroke velocity in the optically paced group (38.9 ± 4.2 V/s vs. 89.6 ± 17.8 V/s in unpaced controls, *Figure 4F*), because TOP is in the steep region of the steady-state inactivation curve where small changes in TOP can have large effects on sodium channel availability and subsequently upstroke velocity.[7] In contrast to a previous publication, expression of *SCN5A* was not altered by chronic pacing[37] (Supplementary material online, *Figure S6*). Interestingly, the spontaneous beating rate was unchanged despite increased DD, which indicates an important role for the depolarized TOP to maintain normal beating rates. It is therefore possible that, despite unchanged SCN5A levels, functionally reduced Na^+ current might be an element of the pacing-induced remodelling, resulting in a more depolarized TOP and decreased upstroke velocity.

In contrast to tachypacing in animal models,[3] which induce cellular hypertrophy, tachypacing of EHTs was associated with smaller cell capacitance. This unexpected finding may be due to the absence of neurohumoral reflex mechanisms upon contractile dysfunction in EHTs *in vitro*. Accordingly, we did not observe different expression of genes known to be involved in hypertrophy (Supplementary material online, *Figure S6*). However, it should be noted that even under *in vitro* conditions, tachypacing of human atrial tissue increased the activity of calcineurin A, expression of calcineurin A regulated transcription factors like NFATc1-4 and several genes involved in hypertrophy.[42] The discrepant findings require further studies. Taken together, chronic optical tachypacing of hiPSC-EHTs induced shortening of contraction, shortening of APD and ERP and more depolarized TOP. Together, these factors favour arrhythmia induction.

4.3 Induction and stability of tachycardia episodes

One of the most interesting findings of this study was the higher arrhythmia vulnerability of EHTs submitted to chronic optical interval pacing. It was previously demonstrated that burst pacing can successfully induce re-entrant arrhythmias in circular cell sheet of hiPSC-CMs[43] and self-terminating non-sustained arrhythmias in cardiopatches.[44] Here we show that burst pacing at 20 Hz can also initiate episodes of tachycardia in EHTs and that the susceptibility to these spontaneous events was higher after chronic optical tachypacing. This might be due to the shorter APD_{90} and ERP of the optically paced ChR2-EHTs. Surprisingly, the

tachycardia episodes showed a long mean duration of 29.8 ± 2.9 min. As previously described,[45] Poincaré plots were measured to assess potential beating irregularities during tachycardia episodes. The stability (Supplementary material online, *Figure S4a*) and the possibility to induce tachycardia episodes several times in the same EHT represent a unique opportunity to test drug efficacy for tachycardia termination. In previous studies,[46] tachycardia was investigated by analysing arrhythmogenesis and calcium abnormalities in hiPSC-CMs obtained from patients suffering from catecholaminergic polymorphic ventricular tachycardia. In this study, we present a 3D tissue composed of hiPSC-CMs in which sustained tachycardia episodes (∼5 Hz) can be induced by burst pacing.

4.4 Mechanism and termination of tachycardia episodes

As described in other models, tachycardia was successfully terminated by overdrive suppression with 20 Hz burst pacing[30] and by optogenetic defibrillation with continuous blue light illumination.[47] Acute pharmacological termination of tachycardia occurred with flecainide (1 µmol/L) in 69% of EHTs.[48] The efficacy may be related to the effect of flecainide on sodium channels, but the ryanodine stabilizing effect of flecainide cannot be ruled out.[49] In order to investigate the mechanism underlying these tachycardia episodes, we analysed the DD of AP recordings during 2 Hz field stimulation. Although, the spontaneous beating rate did not significantly change after chronic optical tachypacing, DD was faster in the optically paced compared to the unpaced ChR2-EHTs (*Figure 6A* and *B*). We observed a positive correlation between DD and tachycardia induction (*Figure 6C*). In a previous publication,[9] we demonstrated almost complete elimination of DD and automaticity by the I_f blocker ivabradine (300 nmol/L) in EHTs beating spontaneously during culture. In contrast, ivabradine (1 µmol/L) was never successful to terminate the tachycardia, even at the high concentration of 1 µmol/L and with at least 15 min exposure time. In line with this finding, mRNA expression of *HCN4*, encoding for the I_f channel, was lower after chronic optical tachypacing (*Figure 6D*). Similar data were previously reported in hiPSC-CMs upon chronic electrical pacing.[12,14] Increased DD was not described in previous studies, even not in Purkinje cells in tachypacing-induced heart failure.[40] These data argue against the role of I_f and point to Ca^{2+}-clock pacemaking mechanisms[50] to underlie the increased DD. In this model we observed a decrease in CASQ2 protein levels (*Figure 6F*). CASQ2 plays a crucial role in calcium-induced calcium release, as it is a calcium binding protein in the sarcoplasmic reticulum (SR). A reduction of CASQ2 and a consequent reduction of Ca^{2+} binding capacity facilitates Ca^{2+}-release and increases the event frequency.[51] At lower level of CASQ2, the SR Ca^{2+} load threshold at which spontaneous Ca^{2+} release happens is lower, increasing the overall probability of arrhythmias.[52] The efficacy of JTV-519 to terminate tachycardia in 46% of EHTs support the hypothesis that altered intracellular Ca^{2+} handling participates in these tachycardia episodes. If this was the mechanism, spontaneous release of Ca^{2+} from the SR causes an elevation of cytosolic Ca^{2+}, activation of the forward mode of NCX and an inward I_{NCX} depolarizing current that depolarizes the cell to a point where the threshold to activate Na channels is reached and an AP activated.[53] However, the limited selectivity of JTV-519[54] suggests that the antiarrhythmic action of the compound may also involve APD prolongation by inhibiting I_{Kr} and I_{K1}. In fact, JTV-519 prolonged ERP in dog atrium[55] but shortened APD in guinea-pig ventricle.[54] In our experiments with tachypaced EHTs, JTV-519 did not significantly prolong APD_{90} in tachypaced EHTs neither in preparations where JTV-519 stopped tachycardia nor in preparations where it was ineffective.

These data do not support the idea that the antiarrhythmic effect of JTV-519 was due to AP prolongation.

Previous studies showed that the selective NCX blocker SEA0400 shortened APD and reduced the incidence of early afterdepolarizations in Langendorff-perfused rabbit ventricles,[56] but the antiarrhythmic potential was inconsistent in the same and other models.[57,58] In our tachycardia model SEA0400 also shortened APD_{90}, but did not suppress burst pacing-induced tachycardia (*Figure 7*). The lack of an antiarrhythmic effect of the NCX blocker is in line with reduced protein level of NCX and argues against a prominent role of NCX-mediated depolarization during tachycardia. Moreover, E-4031 was effective in terminating tachycardia episodes in optically paced EHTs, which might argue rather for reentry as tachycardia mechanism.

In conclusion, we established an optogenetic 3D model with hiPSC-EHTs which allows light pacing with simultaneous force measurements over several weeks. Chronic optical tachypacing-induced functional and molecular remodelling associated with a high vulnerability to burst pacing-induced tachycardia. The effectiveness of classical (flecainide) and experimental (JTV-519 and E-4031) compounds to terminate the tachycardia indicates that this model will be valuable in studying mechanisms of ventricular tachycardia in a human cardiac myocyte context.

5. Limitation

The mechanism underlying tachycardia episodes in this model might be different from the *in vivo* mechanism due to electrophysiological differences and to the lack of a regulatory system in our model. Pulse duration and waveform of the chronic intermittent tachypacing were fixed during this study. It would be interesting to investigate the effect of different pacing time and rate on electrical remodelling. The episodes of tachycardia are self-terminating after 30 min from induction, therefore it would not be possible to test long latency drugs. Proteomics and ion channel remodelling could be analysed to further investigate the effects of chronic optical tachypacing.

Supplementary material

Supplementary material is available at *Cardiovascular Research* online.

Authors' contributions

Acknowledgements

References

1. Wijffels M, Kirchhof C, Dorland R, Allessie MA. Atrial fibrillation begets atrial fibrillation: a study in awake chronically instrumented goats. *Circulation* 1995;**92**:1954–1968.
2. Morillo CA, Klein GJ, Jones DL, Guiraudon CM. Chronic rapid atrial pacing: structural, functional, and electrophysiological characteristics of a new model of sustained atrial fibrillation. *Circulation* 1995;**91**:1588–1595.
3. Han W, Chartier D, Li D, Nattel S. Ionic remodeling of cardiac Purkinje cells by congestive heart failure. *Circulation* 2001;**104**:2095–2100.
4. Kaab S, Nuss HB, Chiamvimonvat N, O'Rourke B, Pak PH, Kass DA, Marban E, Tomaselli GF. Ionic mechanism of action potential prolongation in ventricular myocytes from dogs with pacing-induced heart failure. *Circ Res* 1996;**78**:262–273.
5. Denayer T, Stöhr T, Van RM. Animal models in translational medicine: validation and prediction. *New Horiz Transl Med* 2014;**2**:5–11.
6. Jost N, Virág L, Comtois P, Ordög B, Szuts V, Seprényi G, Bitay M, Kohajda Z, Koncz I, Nagy N, Szél T, Magyar J, Kovács M, Puskás LG, Lengyel C, Wettwer E, Ravens U, Nánási PP, Papp JG, Varró A, Nattel S. Ionic mechanisms limiting cardiac repolarization reserve in humans compared to dogs. *J Physiol* 2013;**591**:4189–4206.
7. Lemoine MD, Mannhardt I, Breckwoldt K, Prondzynski M, Flenner F, Ulmer B, Hirt MN, Neuber C, Horváth A, Kloth B, Reichenspurner H, Willems S, Hansen A, Eschenhagen T, Christ T. Human iPSC-derived cardiomyocytes cultured in 3D engineered heart tissue show physiological upstroke velocity and sodium current density. *Sci Rep* 2017;**7**:5464.
8. Horváth A, Lemoine MD, Löser A, Mannhardt I, Flenner F, Uzun AU, Neuber C, Breckwoldt K, Hansen A, Girdauskas E, Reichenspurner H, Willems S, Jost N, Wettwer E, Eschenhagen T, Christ T. Low resting membrane potential and low inward rectifier potassium currents are not inherent features of hiPSC-derived cardiomyocytes. *Stem Cell Rep* 2018;**10**:822–833.
9. Lemoine MD, Krause T, Koivumäki JT, Prondzynski M, Schulze ML, Girdauskas E, Willems S, Hansen A, Eschenhagen T, Christ T. Human induced pluripotent stem cell-derived engineered heart tissue as a sensitive test system for QT prolongation and arrhythmic triggers. *Circ Arrhythm Electrophysiol* 2018;**11**:e006035.
10. Blazeski A, Renjun Z, Hunter DW, Weinberg SH, Zambidis ET, Tung L. Cardiomyocytes derived from human induced pluripotent stem cells as models for normal and diseased cardiac electrophysiology and contractility. *Prog Biophys Mol Biol* 2012;**110**:166–177.
11. Karakikes I, Ameen M, Termglinchan V, Wu JC. Human induced pluripotent stem cell-derived cardiomyocytes: insights into molecular, cellular, and functional phenotypes. *Circ Res* 2015;**117**:80–88.
12. Hirt MN, Boeddinghaus J, Mitchell A, Schaaf S, Börnchen C, Müller C, Schulz H, Hubner N, Stenzig J, Stoehr A, Neuber C, Eder A, Luther PK, Hansen A, Eschenhagen T. Functional improvement and maturation of rat and human engineered heart tissue by chronic electrical stimulation. *J Mol Cell Cardiol* 2014;**74**:151–161.
13. Nunes SS, Miklas JW, Liu J, Aschar-Sobbi R, Xiao Y, Zhang B, Jiang J, Massé S, Gagliardi M, Hsieh A, Thavandiran N, Laflamme MA, Nanthakumar K, Gross GJ, Backx PH, Keller G, Radisic M, Masse S, Gagliardi M, Hsieh A, Thavandiran N, Laflamme MA, Nanthakumar K, Gross GJ, Backx PH, Keller G, Radisic M. Biowire: a platform for maturation of human pluripotent stem cell-derived cardiomyocytes. *Nat Methods* 2013;**10**:781–787.
14. Ronaldson-Bouchard K, Ma SP, Yeager K, Chen T, Song LJ, Sirabella D, Morikawa K, Teles D, Yazawa M, Vunjak-Novakovic G. Advanced maturation of human cardiac tissue grown from pluripotent stem cells. *Nature* 2018;**556**:239–243.
15. Cui C, Geng L, Shi J, Zhu Y, Yang G, Wang Z, Wang J, Chen M. Structural and electrophysiological dysfunctions due to increased endoplasmic reticulum stress in a long-term pacing model using human induced pluripotent stem cell-derived ventricular cardiomyocytes. *Stem Cell Res Ther* 2017;**8**:109.
16. Geng L, Wang Z, Cui C, Zhu Y, Shi J, Wang J, Chen M. Rapid electrical stimulation increased cardiac apoptosis through disturbance of calcium homeostasis and mitochondrial dysfunction in human induced pluripotent stem cell-derived cardiomyocytes. *Cell Physiol Biochem* 2018;**47**:1167–1180.
17. Zhang C, He D, Ma J, Tang W, Waite TD. Faradaic reactions in capacitive deionization (CDI)—problems and possibilities: a review. *Water Res* 2018;**128**:314–330.
18. Humayun MS, Weiland JD, Chader G, Greenbaum E. *Artificial Sight: Basic Research, Biomedical Engineering, and Clinical Advances*. New York: Springer, 2007.
19. Boyle PM, Karathanos TV, Trayanova NA. 'Beauty is a light in the heart': the transformative potential of optogenetics for clinical applications in cardiovascular medicine. *Trends Cardiovasc Med* 2015;**25**:73–81.
20. Bruegmann T, Malan D, Hesse M, Beiert T, Fuegemann CJ, Fleischmann BK, Sasse P. Optogenetic control of heart muscle in vitro and in vivo. *Nat Methods* 2010;**7**:897–900.
21. Bingen BO, Engels MC, Schalij MJ, Jangsangthong W, Neshati Z, Feola I, Ypey DL, Askar SFA, Panfilov AV, Pijnappels DA, Vries AD. Light-induced termination of spiral wave arrhythmias by optogenetic engineering of atrial cardiomyocytes. *Cardiovasc Res* 2014;**104**:194–205.
22. Mannhardt I, Breckwoldt K, Letuffe-Brenière D, Schaaf S, Schulz H, Neuber C, Benzin A, Werner T, Eder A, Schulze T, Klampe B, Christ T, Hirt MN, Huebner N, Moretti A, Eschenhagen T, Hansen A. Human engineered heart tissue: analysis of contractile force. *Stem Cell Rep* 2016;**7**:29–42.
23. Breckwoldt K, Letuffe-Brenière D, Mannhardt I, Schulze T, Ulmer B, Werner T, Benzin A, Klampe B, Reinsch MC, Laufer S, Shibamiya A, Prondzynski M, Mearini G, Schade D, Fuchs S, Neuber C, Krämer E, Saleem U, Schulze ML, Rodriguez ML, Eschenhagen T, Hansen A. Differentiation of cardiomyocytes and generation of human engineered heart tissue. *Nat Protoc* 2017;**12**:1177–1197.
24. Bazett HC. An analysis of the time-relations of electrocardiograms. *Ann Noninvasive Electrocardiol* 1997;**2**:177–194.
25. Marta L, Ulmer BM, Lemoine MD, Zech ATL, Flenner F, Ravens U, Reichenspurner H, Rol-Garcia M, Smith G, Hansen A, Christ T, Eschenhagen T. Atrial-like engineered heart tissue: an in vitro model of the human atrium. *Stem Cell Rep* 2018;**11**:1–13.
26. Lin JY. A user's guide to channelrhodopsin variants. *Exp Physiol* 2011;**96**:19–25.
27. Clasen L, Eickholt C, Angendohr S, Jungen C, Shin D-I, Donner B, Furnkranz A, Kelm M, Klocker N, Meyer C, Makimoto H. A modified approach for programmed electrical stimulation in mice: inducibility of ventricular arrhythmias. *PLoS One* 2018;**13**:e0201910.
28. Volosin KJ, Beauregard LAM, Fabiszewski R, Mattingly H, Waxman HL. Spontaneous changes in ventricular tachycardia cycle length. *J Am Coll Cardiol* 1991;**17**:409–414.
29. Piskorski J, Guzik P. Geometry of the Poincaré plot of RR intervals and its asymmetry in healthy adults. *Physiol Meas* 2007;**28**:287–300.
30. Fisher JD, Mehra R, Furman S. Termination of ventricular tachycardia with bursts of rapid ventricular pacing. *Am J Cardiol* 1978;**41**:94–102.
31. Crocini C, Ferrantini C, Coppini R, Scardigli M, Yan P, Loew LM, Smith G, Cerbai E, Poggesi C, Pavone FS, Sacconi L. Optogenetics design of mechanistically-based stimulation patterns for cardiac defibrillation. *Sci Rep* 2016;**6**:1–7.
32. Nyns ECA, Kip A, Bart CI, Plomp JJ, Zeppenfeld K, Schalij MJ, Vries AD, Pijnappels DA. Optogenetic termination of ventricular arrhythmias in the whole heart: towards biological cardiac rhythm management. *Eur Heart J* 2017;**38**:2132–2136.
33. Majumder R, Feola I, Teplenin AS, Antoine AF, Vries D, Pan AV, Pijnappels DA. Optogenetics enables real-time spatiotemporal control over spiral wave dynamics in an excitable cardiac system. *Elife* 2018;**7**:e41076.
34. Lapp H, Bruegmann T, Malan D, Friedrichs S, Kilgus C, Heidsieck A, Sasse P. Frequency-dependent drug screening using optogenetic stimulation of human iPSC-derived cardiomyocytes. *Sci Rep* 2017;**7**:1–12.
35. Li Q, Ni RR, Hong H, Goh KY, Rossi M, Fast VG, Zhou L. Electrophysiological properties and viability of neonatal rat ventricular myocyte cultures with inducible ChR2 expression. *Sci Rep* 2017;**7**:1–12.
36. Zamani A, Sakuragi S, Ishizuka T, Yawo H. Kinetic characteristics of chimeric channelrhodopsins implicate the molecular identity involved in desensitization. *Biophysics* 2017;**14**:13–22.
37. Eng G, Lee BW, Protas L, Gagliardi M, Brown K, Kass RS, Keller G, Robinson RB, Vunjak-Novakovic G. Autonomous beating rate adaptation in human stem cell-derived cardiomyocytes. *Nat Commun* 2016;**7**:10312.
38. Schotten U, Haase H, Frechen D, Greiser M, Stellbrink C, Vazquez-Jimenez JF, Morano I, Allessie MA, Hanrath P. The L-type Ca^{2+}-channel subunits α1C and β2 are not downregulated in atrial myocardium of patients with chronic atrial fibrillation. *J Mol Cell Cardiol*. 2003;**35**:437–443.
39. Qi XY, Yeh YH, Xiao L, Burstein B, Maguy A, Chartier D, Villeneuve LR, Brundel B, Dobrev D, Nattel S. Cellular signaling underlying atrial tachycardia remodeling of L-type calcium current. *Circ Res* 2008;**103**:845–854.

40. Han W, Zhang L, Schram G, Nattel S. Properties of potassium currents in Purkinje cells of failing human hearts. *Am J Physiol Heart Circ Physiol* 2002;**283**:H2495–H2503.

41. Lester WC, Schroder EA, Burgess DE, Yozwiak D, Andres DA, Satin J. Steady-state coupling of plasma membrane calcium entry to extrusion revealed by novel L-type calcium channel block. *Cell Calcium* 2008;**44**:353–362.

42. Bukowska A, Lendeckel U, Hirte D, Wolke C, Striggow F, Rohnert P, Huth C, Klein HU, Goette A. Activation of the calcineurin signaling pathway induces atrial hypertrophy during atrial fibrillation. *Cell Mol Life Sci* 2006;**63**:333–342.

43. Shaheen N, Shiti A, Huber I, Shinnawi R, Arbel G, Gepstein A, Setter N, Goldfracht I, Gruber A, Chorna SV, Gepstein L. Human induced pluripotent stem cell-derived cardiac cell sheets expressing genetically encoded voltage indicator for pharmacological and arrhythmia studies. *Stem Cell Rep* 2018;**10**:1879–1894.

44. Shadrin IY, Allen BW, Qian Y, Jackman CP, Carlson AL, Juhas ME, Bursac N. Cardiopatch platform enables maturation and scale-up of human pluripotent stem cell-derived engineered heart tissues. *Nat Commun* 2017;**81**:1825.

45. Brennan M, Palaniswami M, Kamen P. Do existing measures of Poincaré plot geometry reflect nonlinear features of heart rate variability? *IEEE Trans Biomed Eng* 2001;**48**: 1342–1347.

46. Maizels L, Huber I, Arbel G, Tijsen AJ, Gepstein A, Khoury A, Gepstein L. Patient-specific drug screening using a human induced pluripotent stem cell model of catecholaminergic polymorphic ventricular tachycardia type 2. *Circ Arrhythm Electrophysiol* 2017;**10**:e004725.

47. Bruegmann T, Boyle PM, Vogt CC, Karathanos TV, Arevalo HJ, Fleischmann BK, Trayanova NA, Sasse P. Optogenetic defibrillation terminates ventricular arrhythmia in mouse hearts and human simulations. *J Clin Invest* 2016;**126**:3894–3904.

48. Pölönen RP, Penttinen K, Swan H, Aalto-Setala K. Antiarrhythmic effects of carvedilol and flecainide in cardiomyocytes derived from catecholaminergic polymorphic ventricular tachycardia patients. *Stem Cells Int* 2018;**2018**:9109503.

49. Hilliard FA, Steele DS, Laver D, Yang Z, Marchand SL, Chopra N, Piston DW, Huke S, Knollmann BC. Flecainide inhibits arrhythmogenic Ca^{2+} waves by open state block of ryanodine receptor Ca^{2+} release channels and reduction of Ca^{2+} spark mass. *J Mol Cell Cardiol* 2010;**48**:293–301.

50. Lakatta EG, Maltsev VA, Vinogradova TM. A coupled SYSTEM of intracellular Ca^{2+} clocks and surface membrane voltage clocks controls the timekeeping mechanism of the heart's pacemaker. *Circ Res* 2010;**106**:659–673.

51. Handhle A, Ormonde CE, Thomas NL, Bralesford C, Williams AJ, Lai FA, Zissimopoulos S. Calsequestrin interacts directly with the cardiac ryanodine receptor luminal domain. *J Cell Sci* 2016;**2**:3983–3988.

52. Faggioni M, Knollmann BC. Calsequestrin 2 and arrhythmias. *Am J Physiol Heart Circ Physiol* 2012;**302**:H1250–H1260.

53. Kane C, Couch L, Terracciano CMN. Excitation–contraction coupling of human induced pluripotent stem cell-derived cardiomyocytes. *Front Cell Dev Biol* 2015;**3**:1–8.

54. Kumagai K, Nakashima H, Gondo N, Saku K. Antiarrhythmic effects of JTV-519, a novel cardioprotective drug, on atrial fibrillation/flutter in a canine sterile pericarditis model. *J Cardiovasc Electrophysiol* 2003;**14**:880–884.

55. Kiriyama K, Kiyosue T, Wang JC, Dohi K, Arita M. Effects of JTV-519, a novel anti-ischaemic drug, on the delayed rectifier K+ current in guinea-pig ventricular myocytes. *Naunyn Schmiedebergs Arch Pharmacol* 2000;**361**:646–653.

56. Milberg P, Pott C, Fink M, Frommeyer G, Matsuda T, Baba A, Osada N, Breithardt G, Noble D, Eckardt L. Inhibition of the Na^+/Ca^{2+} exchanger suppresses torsades de pointes in an intact heart model of long QT syndrome-2 and long QT syndrome-3. *Heart Rhythm* 2008;**5**:1444–1452.

57. Farkas AS, Makra P, Csík N, Orosz S, Shattock MJ, Fülöp F, Forster T, Csanády M, Papp JG, Varró A, Farkas A. The role of the Na^+/Ca^{2+} exchanger, I Na and I CaL in the genesis of dofetilide-induced torsades de pointes in isolated, AV-blocked rabbit hearts. *Br J Pharmacol* 2009;**156**:920–932.

58. Zhao Z, Wen H, Fefelova N, Allen C, Baba A, Matsuda T, Xie L-H. Revisiting the ionic mechanisms of early afterdepolarizations in cardiomyocytes: predominant by Ca waves or Ca currents? *Am J Physiol Heart Circ Physiol* 2012;**302**:H1636–H1644.